University of Huddersfield Repository

Zhang, Ruiliang, Gu, Fengshou, Mansaf, Haram, Wang, Tie and Ball, Andrew D.

Gear wear monitoring by modulation signal bispectrum based on motor current signal analysis

Original Citation

Zhang, Ruiliang, Gu, Fengshou, Mansaf, Haram, Wang, Tie and Ball, Andrew D. (2017) Gear wear monitoring by modulation signal bispectrum based on motor current signal analysis. Mechanical Systems and Signal Processing, 94. pp. 202-213. ISSN 08883270

This version is available at http://eprints.hud.ac.uk/id/eprint/31496/

Gear Wear Monitoring by Modulation Signal Bispectrum based Motor Current Signal Analysis

Ruiliang Zhang[1], Fengshou Gu[1, 2, #], Haram Mansaf[2], Tie Wang[1,] Andrew D. Ball[2]

[1] School of Mechanical Engineering, Taiyuan University of Technology, Taiyuan, China, 030024
[2] Centre for Efficiency and Performance Engineering, University of Huddersfield, Huddersfield, UK, HD1 3DH.
[#] Corresponding Author / E-mail: f.gu@hud.ac.uk, Tel.: +44 1474 473548; fax: +44 1484 473075.

Abstract: Gears are important mechanical components for power transmissions. Tooth wear is one of the most common failure modes, which can present throughout a gear's lifetime. It is significant to accurately monitor gear wear progression in order to take timely predictive maintenances. Motor current signature analysis (MCSA) is an effective and non-intrusive approach which is able to monitor faults from both electrical and mechanical systems. However, little research has been reported in monitoring the gear wear and estimating its severity based on MCSA. This paper presents a novel gear wear monitoring method through a modulation signal bispectrum based motor current signal analysis (MSB-MCSA). For a steady gear transmission, it is inevitable to exist load and speed oscillations due to various errors including wears. These oscillations can induce small modulations in the current signals of the driving motor. MSB is particularly effective in characterising such small modulation signals. Based on these understandings, the monitoring process was implemented based on the current signals from a run-to-failure test of an industrial two stages helical gearbox under a moderate accelerated fatigue process. At the initial operation of the test, MSB analysis results showed that the peak values at the bifrequencies of gear rotations and the power supply can be effective monitoring features for identifying faulty gears and wear severity as they exhibit agreeable changes with gear loads. A monotonically increasing trend established by these features allows a clear indication of the gear wear progression. The dismantle inspection at 477 hours of operation, made when one of the monitored features is about 123% higher than its baseline, has found that there are severe scuffing wear marks on a number of tooth surfaces on the driving gear, showing that the gear endures a gradual wear process during its long test operation. Therefore, it is affirmed that the MSB-MSCA approach proposed is reliable and accurate for monitoring gear wear deterioration.

Keywords: Motor current signal analysis; Modulation signal bispectrum; Gear wear; Gearbox monitoring.

1. Introduction

Gears are commonly used as a means of power transmission in many industrial applications. Gear wear is a progressive material loss from contacting tooth surfaces, which is an inevitable phenomenon in the service lifetime of gears. Apart from the direct material loss, surface wear also affect significantly time-varying meshing stiffness [1-5], dynamic transmission error [4-6], and load fluctuation [4, 5, 7, 8]. As one of the major failure modes of gears, severe wear can lead to the occurrence of other types of gear failures such as surface pitting, scuffing and broken teeth [9]. Therefore, the subject of gear wear monitoring and diagnosis is receiving a lot of attention in the field of condition monitoring (CM).

For gear wear monitoring, the wear debris analysis is mostly used [9-10], and there is an endeavor for its replacement by more popular vibration monitoring techniques [10-12] and acoustics analysis [13]. The wear debris analysis is carried out off-line and time-consuming. Moreover, wear particles analysis cannot timely reveal changes in gear transmission dynamic features, which can be used to examine if gears still work properly. Vibration based methods have several drawbacks, such as significant signal background noise caused by external excitations, over-sensitive to resonance distortions, and invasive measurements. Similarly, the noise signature is also affected by the interfering sources, transmission paths and background noise [13]. The above mentioned methods also require accessibility to the gearbox, either to collect samples or to mount the transducers on or near the gearbox.

To avoid these shortages of prevalent techniques, the motor current signature analysis (MCSA) for the CM of motor-operated gearbox [14-20] has received growing attention in recent years and achieved considerable advancements. These publications show many interesting achievements in this direction. In all these publications, the use of MCSA for the detection of gear faults has been limited in that no deterministic approaches have been demonstrated. One of the main reasons for this lack of diagnostic clarity is that the harmonic content and noise contained within the real measured signals are high or the fault signals are low. Moreover, the gear transmission system usually produces significant nonlinear coupling phenomenon that will present sum and difference frequency components when the failure occurs. The methods such as fast Fourier transform [14-15] and power spectrum analysis [16] used in the above mentioned achievements, are based on stationary signals and are difficult to solve the nonlinear phenomenon and suppress noises. As a result they can be insufficient to properly correlate the stator current data with faulted conditions. Therefore, many researchers have investigated alternative signal analysis methods, such as empiric mode decomposition (EMD) [17], wavelet demodulation analysis [18] and combined methods [19-20], for analysing current signals for more accurate feature extraction. Although these efforts have shown promising results, they may be still deficient because these signal analysis methods possess limited noise reduction capability.

Higher order spectra (HOS) are useful signal processing tools that have shown significant benefits over traditional spectral analyses because HOS have unique properties of nonlinear system identification, Gaussian noise elimination and phase information retention [21-25]. Therefore, HOS analysis has received high concentrations. In [26], conventional bispectrum (CB) was applied to motor current signals for detecting different degrees of tooth breakage of a two-stage helical gearbox. Ref. [27] introduced MSB which is a significant improvement of the CB in that it enhanced CB to apply the modulation signal efficiently. The results showed reliable fault diagnosis and revealed that random noise can be suppressed effectively, being much better than that of the power spectrum (PS) and CB for diagnosing different seeded faults, such as tooth breakage and shaft misalignment. However, MSB method has not been evaluated for gear wear monitoring and severity assessment, which may be more challenging as the wear may induce current signatures far weaker than tooth breakages.

To examine the performance and extend the applications of using MSB based MCSA to the monitoring of gearboxes, this paper investigates monitoring the deterioration process of an industrial multi-stage helical gearbox based on motor current measurements and MSB analysis. It applies MSB to current signals measured progressively from a run-to-failure experiment to obtain accurate modulation characteristics and their evolution behaviours with operating times, and thereby implementing the gear wear monitoring and severity evaluation. The paper has four sections. Section 2 presents the theoretical basis of gear wear detection based on the MSB-MCSA. Section 3 describes the run-to-failure experimental setups for validating the proposed method. Then, section 4 shows the monitoring results in conjunction with critical interpretations and finally, section 5 is the conclusion.

2 Theoretical basis of gear wear detection based on MSB-MCSA

2.1 Motor Current Model for Gearbox Condition Assessment

When a motor driving mechanical transmission such as a gearbox is operating under healthy conditions, the ideal electromagnetic relationship of the driving motor can be examined by using just one of the three phases. To simplify analysis process, the electromagnetic relationships are examined in phase A and the higher harmonics in the phase is not considered. Referring to supply voltage, the current signal in phase A for a healthy motor drive can be expressed as

$$i_A = \sqrt{2}I\cos(2\pi f_s t - \alpha_I) \tag{1}$$

Correspondingly, the magnetic flux in the motor stator is

$$\varphi_A = \sqrt{2}\varphi\cos(2\pi f_s t - \alpha_\varphi) \tag{2}$$

The electrical torque produced by the interaction between the current and flux can be expressed as

$$T = 3P\varphi I \sin(\alpha_I - \alpha_\varphi) \tag{3}$$

where I and φ denote the root mean squared (RMS) amplitudes of the supply current and the linkage flux respectively, α_I and α_ϕ are the phases of the current and flux respectively referring to the phase of supply voltage signal, f_s is the fundamental frequency of the electrical supply and P is the number of pole pairs.

Gear supporting systems usually have much higher stiffness, compared with gear dynamics systems. Tooth friction and wear can be regarded as one of the main sources corresponding to the changes in dynamic load [4]. Whenever there is a load fluctuation, there will be an additional torque component oscillating at rotating frequency around the electrical torque [28]. Gu et al. [27] have derived the effect of a single rotating frequency additional torque on the stator current. Hence, the effect of additional torque only relating to rotating frequencies have been considered in this article while deriving the resultant current signal in phase A, which is an extension of the derivation given in [27].

The total additional torques ΔT in the induction motor consist of some additional oscillatory torques ΔT_k at corresponding rotational frequency f_k with respect to current amplitude I_k and phase α_k given by Eq. (4)

$$\Delta T = \sum_{k=1}^{n} \Delta T_k \tag{4a}$$

$$\Delta T_k = 3P\varphi I_k \sin[2\pi f_k t - (\alpha_\varphi - \alpha_k)] \tag{4b}$$

where k is the number of shafts in the downstream gearbox. The oscillatory torques cause corresponding angular variation is

$$\Delta \beta_k = \frac{3P^2 \varphi I_k}{4\pi^2 f_k^2 J} \sin[2\pi f_k t - (\alpha_\varphi - \alpha_k)] \tag{5}$$

where J is the inertia of the rotor system. This angular oscillation produces phase modulation to the linkage flux in Eq. (2) and yields

$$\varphi_A^k = \sqrt{2}\varphi \cos[2\pi f_s t - \alpha_\varphi - \Delta\beta_k)] \tag{6}$$

Considering $\Delta\beta_k$ is very small, leading to approximates: $\cos(\Delta\beta_k) \approx 1$ and $\sin(\Delta\beta_k) \approx \Delta\beta_k$, the linkage flux now can be simplified and examined in three modulated components explicitly:

$$
\begin{aligned}
\varphi_A^k &\approx \sqrt{2}\varphi \cos(2\pi f_s t - \alpha_\varphi) + \sqrt{2}\varphi\Delta\beta_k \sin(2\pi f_s t - \alpha_\varphi) \\
&= \sqrt{2}\varphi\cos(2\pi f_s t - \alpha_\varphi) \\
&\quad + \frac{\sqrt{2}}{2}\varphi\Delta\varphi_k \cos[2\pi(f_s - f_k)t - \alpha_k] + \frac{\sqrt{2}}{2}\varphi\Delta\varphi_k \cos[2\pi(f_s + f_k)t - 2\alpha_\varphi - \alpha_k + \pi]
\end{aligned}
\tag{7}
$$

where $\Delta\varphi_k = \dfrac{3P^2 \varphi I_k}{4\pi^2 f_k^2 J}$. The derivative of the first term of the flux in Eq. (7) is the fundamental electromagnetic force (EMF).

By comparing Eq. (7) and Eq. (2), the change of linkage flux can be obtained as

$$\Delta\phi_A^k = \frac{\sqrt{2}}{2}\phi\Delta\varphi_k \{\cos[2\pi(f_s - f_k)t - \alpha_k] + \cos[2\pi(f_s + f_k)t - 2\alpha_\varphi - \alpha_k + \pi]\} \tag{8}$$

Eq. (8) shows that the change of flux contains two sidebands around the fundamental frequency, each having different phases. This linkage flux will produce new electromagnetic forces (EMFs) and hence induce the corresponding additional current signals in the stator based on the motor equivalent circuit [29] as follows:

$$\Delta i_A^k = \frac{\sqrt{2}}{2} I_{lk} \cos[2\pi(f_s - f_k)t - \alpha_I - \alpha_k - \phi_k] + \frac{\sqrt{2}}{2} I_{rk} \cos[2\pi(f_s + f_k)t - \alpha_I - 2\alpha_\varphi - \alpha_k - \phi_k + \pi] \tag{9}$$

where ϕ_k is the angular displacement of motor equivalent circuit impedance at supply frequency, I_{lk} and I_{rk} are the RMS values of the lower sideband component and the upper sideband component, respectively. Combining Eq. (1) with Eq. (9) yields the final current signal under the condition of the wear in multi-stage gearbox:

$$i_A^F = i_A + \sum_{k=1}^{n} \Delta i_A^k$$

$$= \sqrt{2}I\cos(2\pi f_s t - \alpha_I)$$

$$+ \sum_{k=1}^{n} \{\frac{\sqrt{2}}{2}I_{lk}\cos[2\pi(f_s - f_k)t - \alpha_I - \alpha_k - \phi_k] + \frac{\sqrt{2}}{2}I_{rk}\cos[2\pi(f_s + f_k)t - \alpha_I - 2\alpha_\varphi - \alpha_k - \phi_k + \pi]\}$$

(10)

As seen from Eq. (10), any torque oscillating with a specific frequency f_k will have sidebands across the supply frequency f_s in the motor current signature. And the phase angles of both sidebands are completely different. Nevertheless, based on the changes in magnitudes and sidebands it is feasible to assess the tooth wear from the gear transmission.

2.2 Modulation Signal Bispectrum

Previous studies [27] has shown the consequence of ignoring phase information using power spectrum may degrade diagnosis performance for the case of incipient faults when the sideband amplitude is very small and masked by various random noises: measurement instruments and additional induction currents induced by environment and random magnetic fields. On the other hand, MSB analysis allows the retention of both the amplitude and the phase information, the suppression of random noise and the identification of nonlinear modulation effects.

For a discrete time current signal $x(t)$ with corresponding Discrete Fourier Transform (DFT) $X(f)$, the MSB can be defined in the frequency domain as [27]

$$B_{MS}(f_k, f_s) = E\left\langle X(f_s + f_k)X(f_s - f_k)X^*(f_s)X^*(f_s)\right\rangle$$

(11)

where f_s and f_k are the carrier or supply frequency and modulation or fault frequency respectively, $X^*(f_s)$ is the complex conjugate of $X(f_s)$ and $E\langle\ \rangle$ denotes the statistical expectation operator, showing that a statistical average operation is necessary for the MSB estimation process and therefore achieve effective noise reduction, which is important to accurately estimate the sideband magnitudes for measuring fault severity.

The overall phase of MSB in Eq. (11) can be calculated by

$$\varphi_{MS}(f_k, f_s) = \varphi(f_s + f_k) + \varphi(f_s - f_k) - \varphi(f_s) - \varphi(f_s)$$

(12)

When two components f_s and f_k are in coupling, their phases are related by

$$\varphi(f_s + f_k) = \varphi(f_s) + \varphi(f_k)$$
$$\varphi(f_s - f_k) = \varphi(f_s) - \varphi(f_k)$$

(13)

By substituting Eq. (13) into Eq. (12) the total phase of MSB will be zero and the amplitude of MSB will be the product of the four magnitudes, which is the maximum of the complex product. Thus, a bispectral peak will appear at bifrequency (f_k, f_s) considering both sidebands simultaneously. This is more accurate and apparent in representing the sideband characteristics of modulation signals.

With this definition, the MSB phase of faulty current signals presented in Eq. (10) can be obtained as

$$\varphi_{MS}(f_k, f_s) = 2\alpha_\varphi + 2\alpha_F + 2\phi_k + \pi$$

(14)

Eq. (14) shows that MSB phase of motor current signals only relates to the sideband component i.e. the angular position of faults and motor design and operation parameters, but excludes the phase of the fundamental component. It means that MSB is independent of the angular position of the rotor or the start point of a signal acquired. This will allow sufficient averages in MSB estimation to be performed using a data set collected or framed at any time. The average in turn will suppress random noise and non-modulating components to obtain a reliable estimation of MSB and of the hidden modulating signals.

The amplitude value of MSB at bifrequency (f_k, f_s) can be denoted as

$$V_k = \left|B_{MS}(f_k, f_s)\right|$$

(15)

This MSB based approach has been shown to yield outstanding performance in characterizing the small modulating components of motor current signals for diagnosing different electrical and mechanical faults [21] [27] [30]. Therefore, it is also based on MSB in this study to extract accurately the amplitude of sidebands in current signals for the purpose of gear wear monitoring and severity detection.

3 Test method

In this paper, a run-to-failure test was carried out to examine gear wear process monitoring through motor current measurements. The test is based on a two-stage gearbox test system as shown in the schematic diagram of Figure 1. The transmission system

consists of a 3-phase AC motor, a two-stage helical gearbox, flexible couplings and a DC motor which acts as a mechanical load. The gearbox is driven by AC drive motor. The required speed and load are approved via a touch screen interface of the resistor bank controller, which sends the required values to both AC motor and DC generator. The induction motor is rated at 11kW at 1470 rpm and controlled by a variable speed drive to operate under different operating conditions. The gearbox under test is also rated at 11kW at 1470 rpm with splash lubrication. The technical specification of the helical gearbox is given in Table 1. To speed up gear failure, the tooth width of the driving gear at the input shaft is halved, as shown in Figure 2. This increases local contact stress by about 40% and is often adopted for an early failure test.
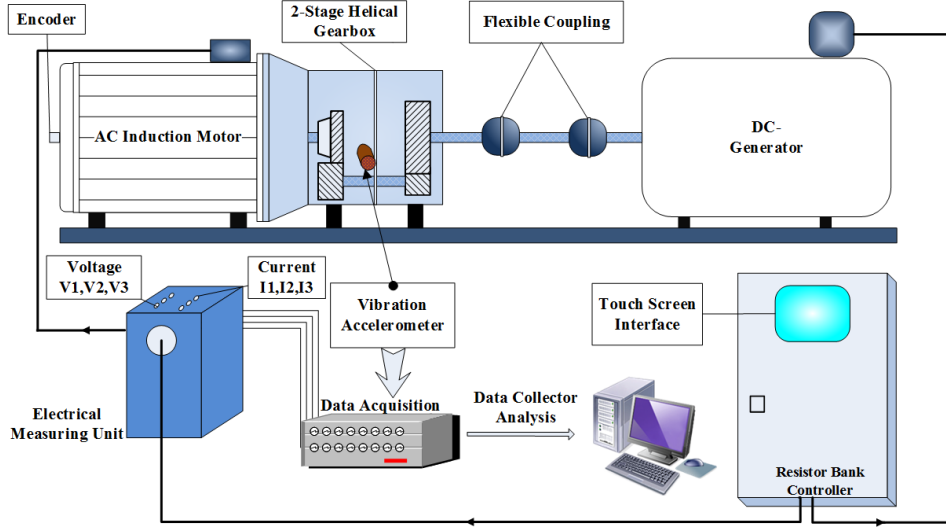

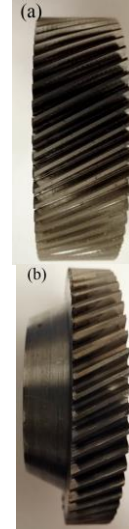**Figure 1** Schematic diagram of test facility

Figure 2 The driving gear of the first stage (a) initial (b) half removed

During the course of the test, both current and vibration signals were continuously recorded with a time interval of 50 minutes, detailed in Figure 3. Electrical current signals are measured by a Hall-effect sensor with the sensitivity of 5A/V and frequency response range of 1Hz to 4000 Hz. A 16-bit resolution data acquisition system with 16 analogy input channels is used to capture and convert the analogy signals acquired from the transducers to digital signals and then transfer to the host computer for post MSB and spectrum analysis. All the measurements are sampled at a rate of 100 kHz and with a data length of 16 seconds at each acquisition. Such a high rate is mainly for a high accuracy of speed calculation based on the encoder pulse train. For MSB based MCSA, the sampling rate can be as low as 5 kHz if the rotor bar passing frequency is interested. In addition, the vibration of gearbox is also measured simultaneously by an accelerometer with a sensitivity 4mv/m/s^2 in order to benchmark the MCSA.

Table 1. Specification of Two-Stage Helical Gearbox

Gear Parameters	1st Stage	2nd Stage
Number of teeth	58/47	13/59
Module (mm)	1.25	2
Pressure angle (deg)	20	20
Helix angle (deg)	27	13
Actual Face width (mm)	13/25	36
Contact ratio	1.45	1.469
Overlap ratio	1.445	1.289
Centre distance (mm)	74	
Meshing frequency (Hz)	$f_{m1} = 1421$	$f_{m2} = 393.04$
Shaft frequency (Hz)	$f_{r1} = 24.5$ $f_{r2} = 30.23$ $f_{r3} = 6.66$	

In order to examine the effect of wear on motor current under different loads, five different operating loads at full speed are applied to the system, as illustrated in Figure 3 below. The test has been conducted with no intermediate installation interruptions to avoid any inevitable installation uncertainty errors.
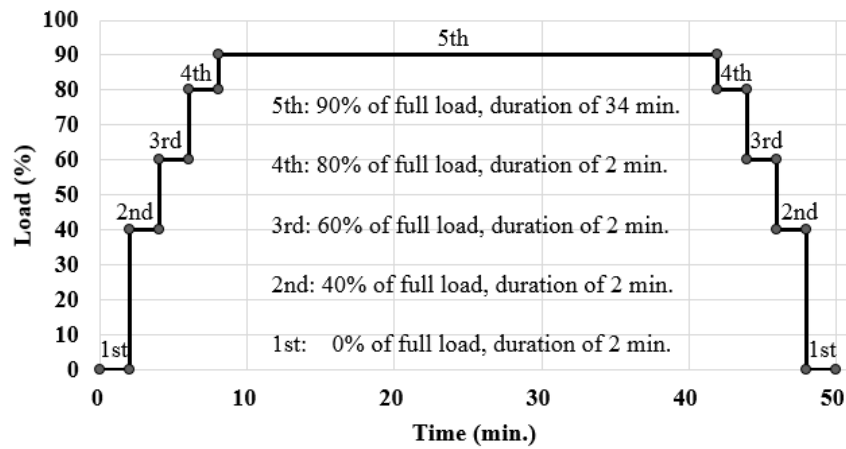
Figure 3 Load and speed in a test operation cycle

The test was terminated after 477 hours, due to a significant increase in the monitored current amplitude, and high vibration level, which indicates there is a clear abnormality occurring in the system. The gearbox was then dismantled and inspected. It has found that clear tooth defects are present on the gear teeth surface as illustrated in Figure 4. It shows that the tooth surface of the driving gear has obvious scuffing markers, as illustrated in Figure 4 (b) and (c) in which excessive wear effect is more significant on the tooth flank below the pitch line, compared with the initial surfaces in Figure 4(a). Moreover, it also shows that the wear marks in Figure 4 (c) look slightly higher, showing non-uniform wear across the circumference of the gear or unsymmetrical wear due to inevitable eccentricity and run-out errors. These phenomenas are typical features caused by the excessive wear under higher contact stress, which are common failures and have been observed in many studies [31-37].
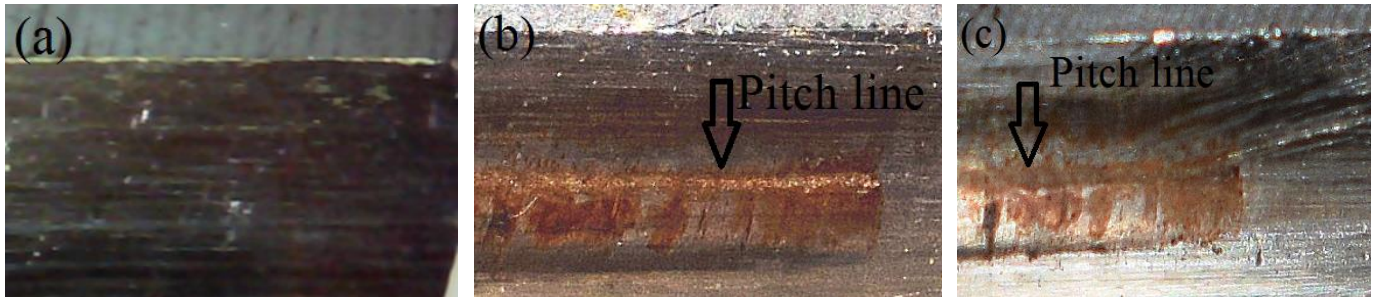

Figure 4 Scuffing on gear teeth of tested gear
(a) initial tooth surface (b) scuffing markers on one tooth surface (c) scuffing markers on the other tooth surface

4 Results and Discussion

In order to evaluate the performance of MSB-MCSA approach in monitoring gear wear progression, the recorded current data are processed using MSB methods in which a 60 times of average is achieved based on the data length. In addition, a Hanning window is applied to the data frame during the fast Fourier transform to suppress spectral leakages.

To find effective diagnosis features, MSB has been calculated up to 3000 Hz, in which the components at the stator slot, rotor bar pass frequencies and the two mesh frequencies can be explored. However, it was observed that the most significant information lies in the range below 35Hz, particularly relating to gear shaft rotation frequencies at which MSB exhibits high amplitudes. This shows high correlation with gearbox operations. As discussed in Section 2, this observation agrees with the view of additional torque components oscillating at rotating frequency. In the meantime, any additional torque changes in the high frequency range can be smoothed significantly by the induction mechanisms as the flux change is inversely proportional to the squared frequency according to (5) and [15, 18, 28]. Therefore, MSB analysis is carried out in a low arrangement up to 80Hz in this study. In addition, to show the power of modulation components, a root squared MSB magnitude is presented according to:

$$A_k = \left| B_{MS}(f_k, f_s) \right|^{0.5} \tag{16}$$

In this paper, A_k at each shaft rotation frequency is selected as the monitoring feature and presented against the operating time to show the gear wear progression and location.

4.1 MSB Characteristics and Monitoring Features

Figure 5 shows representative results of MSB for the current signals in early operating periods, specifically at the 4th hour, under the different load levels in the run-to-failure test. In the graphs, there are three distinctive peaks at the supply frequency of 50 Hz for all load cases. In particular, A_{r1} and A_{r2} are very dominant. These components correspond to the first two rotational frequencies of $f_{r1} = 24.3$ Hz and $f_{r2} = 29.8$ Hz respectively. Thus they reflect the dynamic behaviour of the gear transmission for the 1st stage of the gearbox. In the meantime, the peak value A_{r3} at $f_{r3} = 6.6$ Hz is also visible, showing that this MSB magnitude can also provide desired information of the transmission dynamics at the second stage. This shows that the testing gearbox exists inherent manufacture errors such as eccentricity and run-out which cause oscillations in speed and loads. In addition, the highest peak is at f_{r1} and the lowest is at f_{r3}, showing that the rational dynamics are very different i.e. the speed fluctuation at the low speed shaft is the lowest even though it may have higher dynamical load. In general, these bispectral peaks show that MSB can reveal the nonlinear interaction between the current signals and the downstream gearbox with its shaft frequencies as the modulating components. This is in agreement with the proposed analysis made in Section 2.1.
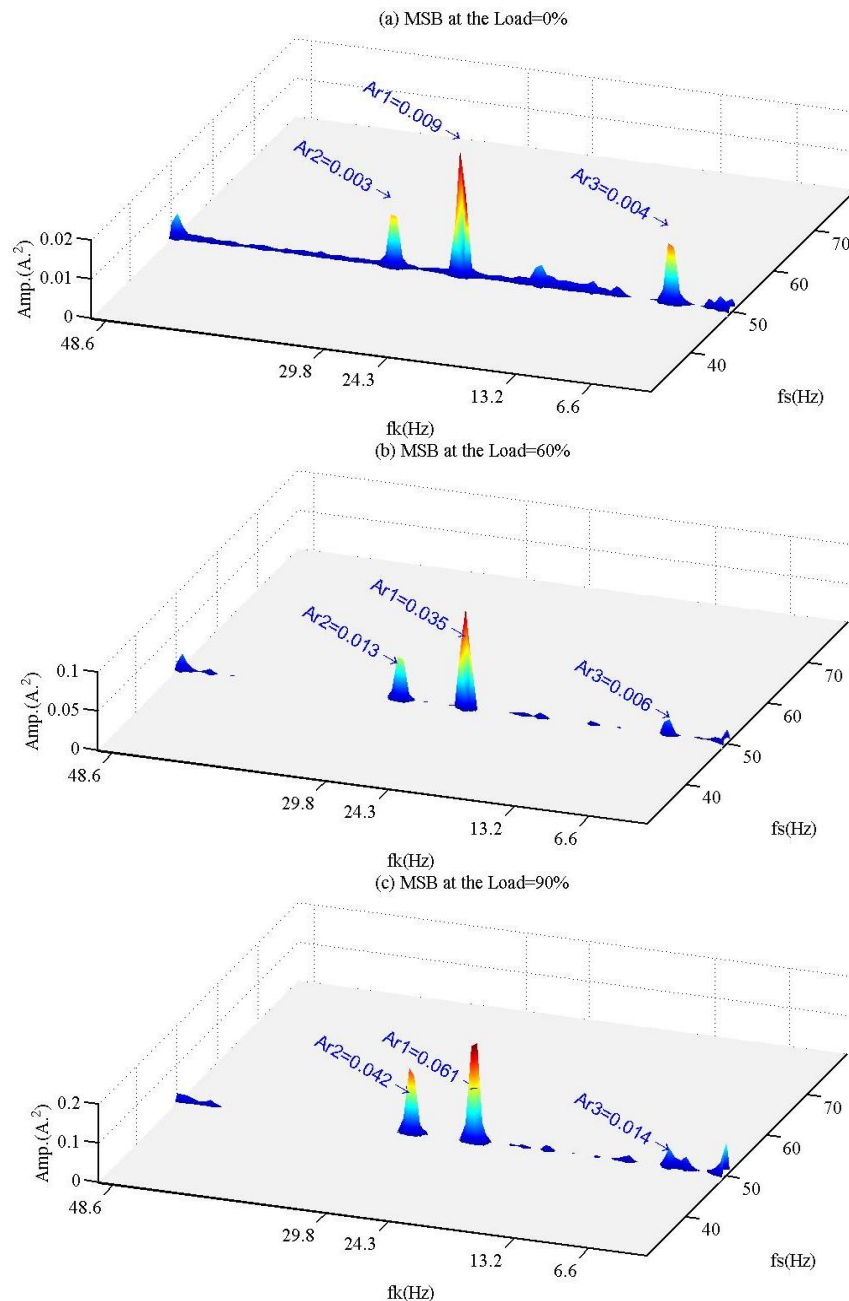

Figure 5 MSB spectrum at the 4th hour under different load cases

Furthermore, it also can be observed clearly from Figure 5 that A_{r1}, A_{r2} and A_{r3} have a clear increase with the load increasing. It shows that the higher loads induce more elastic deformations to both the tooth profiles and the gear supporting system and thereby severer modulation to the supply components. This shows that these peaks are very sensitive to gear loads. Moreover, any gear faults either local tooth breakages or distributed gear wears can cause increases in not only dynamic loads but also static loads. Consequently, these peaks will also increase to reflect these load changes. This is consistent with the fault symptoms that appear to be more clearly pronounced at a higher load than a lower load condition [26].

In Addition, Figure 5 also shows that MSB slices at f_s =50Hz can provide sufficient information to characterize the modulations due to gear dynamic effect. Therefore, only peaks appearing at this slice will be extracted in establishing the diagnostic features. This also shows that using one MSB slice for wear monitoring will reduce computational work significantly and hence the method can be implemented on-line.
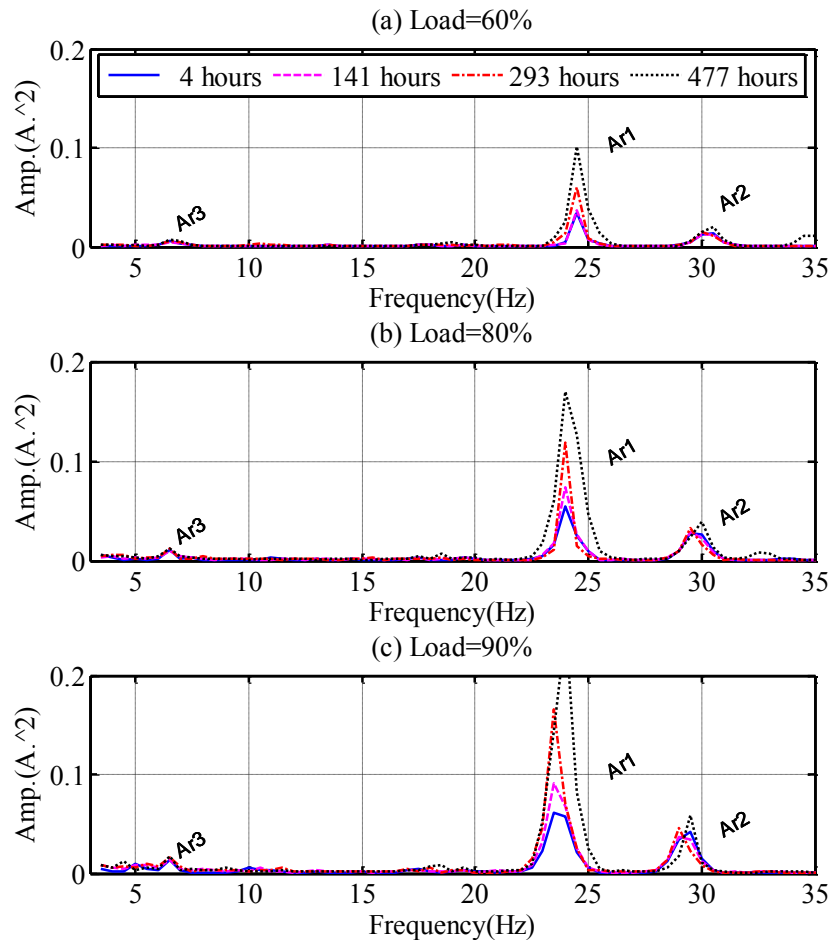

Figure 6 MSB slice of 50 Hz at different operating times under different loads

Figure 6 shows the MSB slices at 50 Hz under three higher loads: 3rd=60%, 4th=80%, and 5th=90% of full load for four increments of operating times: 4 hours, 141 hours, 293 hours, and 477 hours. By comparing them across the operating times, it can be found that the amplitudes of A_{r1} have a clear increase, indicating that wear produces higher nonlinear interaction between the input shaft frequency f_{r1} and the fundamental supply component and hence shows the higher load oscillations due to gear wear accumulated over the operating period. At the same time, the amplitudes of A_{r2} also show a slight increase. Moreover, the amplitudes of A_{r3} keep constant throughout the whole period. These change patterns of MSB peaks show that the gear wear is much severer on the first shaft, that is the testing driving gear shows severe wear defects, which are illustrated in Figure 4 (b) and (c). Therefore, the MSB peaks can be based to locate which gear is faulty and assess the degree of the wear severity.

4.2 MSB-MCSA based Wear Severity Monitoring

Based on aforementioned analysis, MSB peaks value at bifrequency (f_k, f_s) can be used to monitor the gear healthy condition. For underline gearbox, there are three rotating shaft frequencies: f_{r1}, f_{r2} and f_{r3} detailed in Table 1. Their MSB peak values can be obtained by

$$A_{r1} = \left| B_{MS}(f_{r1}, f_s) \right|^{0.5}$$
$$A_{r2} = \left| B_{MS}(f_{r2}, f_s) \right|^{0.5}$$
$$A_{r3} = \left| B_{MS}(f_{r3}, f_s) \right|^{0.5} \tag{17}$$

Figure 7 shows the monitoring trends of A_{r1}, A_{r2} and A_{r3} respectively under the three higher loads (3rd=60%, 4th=80%, and 5th =90% of full load). It can be clearly seen from Figure 7 that there are obvious differences in the trend between the worn and baseline operations, especially for all three higher load operations. A_{r1} increases slowly to the peak at the 20th hour of operation, and then fluctuates and drops slightly to a lower level at the 52nd hour. From the 52nd hour onwards, the peak values exhibit a steady increasing trend, showing that the gear deterioration exhibits a steady enlargement but with different rates.

The slow changes in peak values in the first 20 hours indicate the gear set experiences the run-in process. In this period the tooth surface asperities are removed. The peak value decreases during 20th-52nd hours of operation. This can be viewed as the gear pair self-modify their profiles through the wear effect. As a result, the run-out errors become less and gear engagement is becoming more conformity. This also clearly indicates that the run-in process occurred during the first 52 hours, which means the gear mesh condition is improved during this period. However, after run-in period, the wear would lead to the gradual deterioration in gear meshing conditions.

The slight increasing trend of peak values from the 52th to 220th hours is a clear indication of the initial wear development, which also is called a mild wear period because it is usually characterized by slow but steady material removal. This then shows that the MSB-MCSA can accurately indicate the occurrence of incipient wear in the driving gear at the first stage of gearbox.

After the 220th hour, the MSB peaks increase more significantly with slight fluctuations, which show the gradual enlargement of the gear wear during this moderate wear period. It also can be seen that the MSB fluctuation becomes higher from about the 411st hour up to the test termination (the 477th hour), which reveals that the gear wear started to be severe at that time due to faster and larger material removals. During this stage of the process, the wear may lead to temporary improved engagements, resulting in smaller oscillations. This behaviour of MSB peaks can indicate severe wear period.

Although A_{r1} MSB peak value of the input shaft exhibits a clear increasing trend, A_{r2} and A_{r3} the other two shafts exhibit very marginal increases throughout the operation course. However, A_{r2} exhibits a relatively clearer increase at the onset of the moderate wear period and during late operations. Comparatively, A_{r3} does not exhibit such increase features, instead it increases with a very slow rate, correspondingly largely to the mild wear process. The average MSB peak values of ten sets selected and beginning (baseline) and the end of operations (termination) for comparison are listed in Table 2. A_{r1} is at least 123% higher than its baseline. A_{r2} increases by 20% and A_{r3} almost remains the same. These results also confirm that there are different wear severity occurring at the identified gear. Therefore, it can be concluded that the tooth wear at the first gear set is significantly more severe and that the second stage of the gearbox is relatively healthy.

Table 2. The average MSB peak values

	Load	Baseline (A^2)	Termination (A^2)	Increase rate (%)
A_{r1}	3rd	0.0358	0.0799	123
	4th	0.0574	0.1498	161
	5th	0.0685	0.2090	205
A_{r2}	3rd	0.0145	0.0176	22
	4th	0.0302	0.0387	28
	5th	0.0452	0.0527	17
A_{r3}	3rd	0.0059	0.0060	2
	4th	0.0106	0.0108	2
	5th	0.0142	0.0139	-2

Based on the above analysis, the change in MSB peaks at different rotational frequencies can be used to determine which gear sets are faulty and how severe the wear progressions are. This gradual steady trend can be used to achieve a high accuracy in predicting the fault advancement for implementing timely maintenances.
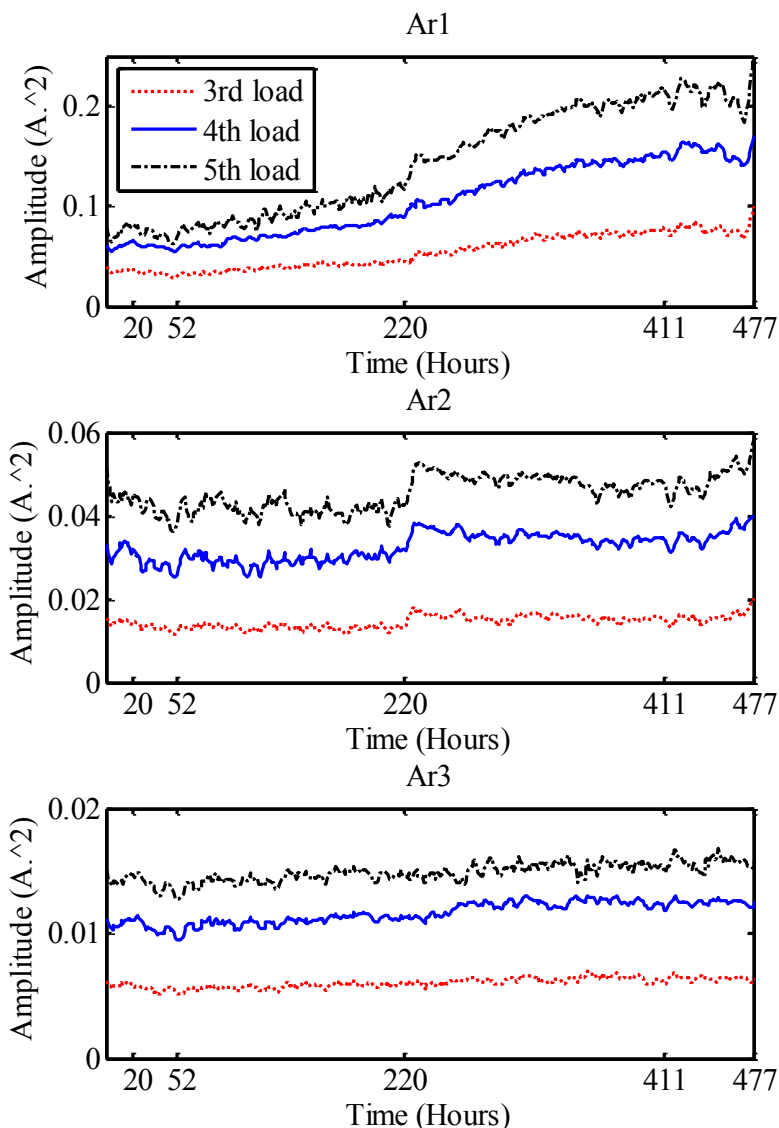

Figure 7 The monitoring trends based on MSB peak values

4.3 Vibration Based Wear Severity Trend

To benchmark the performance of the MSB-MCSA based gear wear monitoring, the vibration signals for the run-to-failure test under the same conditions were also collected using one accelerometer mounted on the gearbox casing close to the tested gear to reduce the vibration influences of the other part and path transitions attenuation, detailed in see Figure 8.

The RMS value which is a common diagnostic feature and used widely for vibration based monitoring is used to monitor wear process. Figure 9 shows the RMS trends for the test period. It can be seen that RMS trends fluctuate greatly with operating time and differ significantly between loads. The trends may provide information to show that the gear is very faulty at late operations such as at 460 hours.

However, they exhibit very large drops at the start of the moderate wear period. This makes it difficult to judge the gear meshing conditions. In addition, there are many local jumps in the trend which will add more uncertainties in implementing condition prognosis. The vibration behaving in these ways show the vibration is very sensitive to the nonlinear effect of gear meshing dynamics and vibration transmission paths [38], which often require significant efforts in signal processing and feature optimization in order to develop a consistent trend for monitoring and prognosis. The authors have tried different methods such as

the popular time synchronous average, wavelet transforms and MSB. Unfortunately, it has not obtained a monitoring trend as good and direct as that of MSB-MCSA.

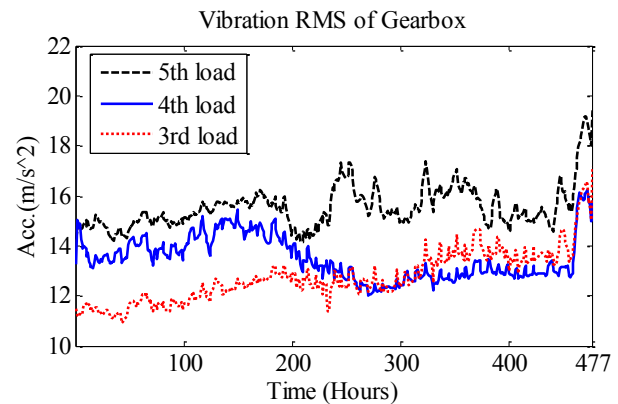**Figure 8** Accelerometer position on gearbox

Figure 9 RMS of the vibration signal for gear wear process

5 Conclusion

Based on this study and results achieved, it can be concluded that MSB-MCSA is an effective approach to non-intrusively and can remotely monitor the slow gear process and diagnose wear severity and fault location of multi-stage helical gearbox. The theoretical analysis shows that the induction motor current signals contain the small modulation components relating to the gearbox wear deterioration process. In particular, tooth wear causes load oscillations, which can be characterised accurately by MSB because MSB possesses the high performance of noise suppression while enhancing the nonlinear effect of modulations, presenting in the conventional power spectrum as the lower and higher sidebands corresponding gear rotating frequency across the supply frequency. In addition, MSCA mainly relies on the information of the torsional dynamics of the gear transmission system. It has been much less influenced by the nonlinearity of translational vibration responses. Therefore, a more steady and consistent monitoring trend can be obtained by MSB-MCSA, allowing a depiction of different gear wear stages and the progressive deterioration.

Acknowledgements

References

[1]. Choy, F. K., Polyshchuk, V., Zakrajsek, J. J., Handschuh, R. F., & Townsend, D. P., Analysis of the effects of surface pitting and wear on the vibration of a gear transmission system, Tribology International. 29 (1) (1996) 77-83.

[2]. Flodin, Anders, and Sören Andersso, Simulation of mild wear in spur gears, Wear. 207 (1) (1997) 16-23.

[3]. Yesilyurt, Isa, Fengshou Gu, and Andrew D. Ball, Gear tooth stiffness reduction measurement using modal analysis and its use in wear fault severity assessment of spur gears, NDT & E International. 36(5) (2003) 357-372.

[4]. Huali Ding, DYNAMIC WEAR MODELS FOR GEAR SYSTEMS, the Ohio State University, Columbus, 2007.

[5]. Liu, Xianzeng, Yuhu Yang, and Jun Zhang, Investigation on coupling effects between surface wear and dynamics in a spur gear system, Tribology International. 101 (2016) 383-394.

[6]. Flodin, Anders, and Sören Andersson, A simplified model for wear prediction in helical gears, Wear. 249 (3) (2001) 285-292.

[7]. Osman, Thaer, and Ph Velex, Static and dynamic simulations of mild abrasive wear in wide-faced solid spur and helical gears, Mechanism and Machine Theory. 45(6) (2010) 911–924.

[8]. Wojnarowski, Jozef, and Valentin Onishchenko, Tooth wear effects on spur gear dynamics, Mechanism and Machine Theory. 38(2) (2003) 161-178.

[9]. P. J. Dempsey, Integrating oil debris and vibration measurement for intelligent machine health monitoring, Glenn Research Center, Cleveland, Tech. Rep. NASA/TM-2003-211307, 2003.

[10]. Hu, Chongqing, Wade A. Smith, Robert B. Randall, and Zhongxiao Peng, Development of a gear vibration indicator and its application in gear wear monitoring, Mechanical Systems and Signal Processing. 76 (2016) 319-336.

[11]. Ziaran, Stanislav, and Radoslav Darula, Determination of the state of wear of high contact ratio gear sets by means of spectrum and cepstrum analysis, Journal of Vibration and Acoustics. 135 (2) (2013) 021008.

[12]. Mathew, J., and J. S. Stecki, Comparison of vibration and direct reading ferrographic techniques in application to high-speed gears operating under steady and varying load conditions, Lubrication engineering. 43 (8) (1987) 646-653.

[13]. Ahmaida, Anwar, Zhen, Dong, Gu, Fengshou and Ball, Andrew, Gear wear process monitoring using acoustic signals, 21st International Congress on Sound and Vibration, Beijing, China, 2014.

[14]. SU, Heng, Mai-sheng HONG, and Shi-bo XIONG, Gears Fault Diagnosis by Monitoring Stator Current, Journal of Shanghai Jiaotong University. 34 (10) (2000):1431-1416.

[15]. Kia, Shahin Hedayati, Humberto Henao, and Gerard-Andre Capolino, Gearbox monitoring using induction machine stator current analysis, In Diagnostics for Electric Machines, Power Electronics and Drives. IEEE International Symposium on. IEEE, Cracow, Poland, (2007) 149-154.

[16]. Kia, Shahin Hedayati, Humberto Henao, and Gérard-André Capolino, A comparative study of acoustic, vibration and stator current signatures for gear tooth fault diagnosis, Electrical Machines (ICEM), XXth International Conference on. IEEE, Marseille, France, (2012) 1514-1519.

[17]. Kia, Shahin Hedayati, Humberto Henao, and Gerard-Andre Capolino, Analytical and experimental study of gearbox mechanical effect on the induction machine stator current signature, IEEE Transactions on Industry Applications. 45 (4) (2009) 1405-1415.

[18]. Kar, Chinmaya, and A. R. Mohanty, Monitoring gear vibrations through motor current signature analysis and wavelet transform, Mechanical systems and signal processing, 20(1) (2006) 158-187.

[19]. Lin, Deng-Fa, Po-Hung Chen, and Mike Williams, Measurement and Analysis of Current Signals for Gearbox Fault Recognition of Wind Turbine, Measurement Science Review. 13(2) (2013) 89-93.

[20]. Rajendra, Barshikar Raghavendra, and Santosh V. Bhaskar, Condition Monitoring of Gear Box by Using Motor Current Signature Analysis, International Journal of Scientific and Research Publications. 3 (8) (2013) 563-568.

[21]. Gu, Fengshou, Yimin Shao, N. Hu, A. Naid, and A. D. Ball, Electrical motor current signal analysis using a modified bispectrum for fault diagnosis of downstream mechanical equipment, Mechanical Systems and Signal Processing. 25 (1) (2011) 360-372.

[22]. Arthur, Neil, and Jim Penman, Induction machine condition monitoring with higher order spectra, IEEE Transactions on Industrial Electronics. 47 (5) (2000) 1031-1041.

[23]. Howard, I. M., Higher-order spectral techniques for machine vibration condition monitoring, Proceedings of the Institution of Mechanical Engineers, Part G: Journal of Aerospace Engineering. 211 (4) (1997) 211-219.

[24]. Kim, Young C., and Edward J. Powers, Digital bispectral analysis and its applications to nonlinear wave interactions. Plasma Science, IEEE Transactions on plasma science. 7(2) (1979) 120-131.

[25]. Chow, T. W. S., and Gou Fei, Three phase induction machines asymmetrical faults identification using bispectrum, IEEE Transactions on Energy Conversion. 10 (4) (1995) 688-693.

[26]. Rgeai, Mohamed Nagi, Helical gearbox fault detection using motor current signature analysis, University of Manchester, Manchester, 2007.

[27]. Chen, Zhi, Tie Wang, Fengshou Gu, Mansaf Haram, and Andrew Ball, Gear Transmission Fault Diagnosis Based on the Bispectrum Analysis of Induction Motor Current Signatures, Journal of Mechanical Engineering. 48 (21) (2012) 84-90.

[28]. Yacamini, R., K. S. Smith, and L. Ran, Monitoring torsional vibrations of electro-mechanical systems using stator currents, Journal of vibration and acoustics. 120 (1) (1998) 72-79.

[29]. F. Filippetti, G. Franceschini, C. Tassoni, AI techniques in induction machines diagnosis including the speed ripple effect, IEEE Transactions on Industry Applications. 34 (1) (1998) 98–108.

[30]. Gu, Fengshou, T. Wang, Ahmed Alwodai, Xiange Tian, Yimin Shao, and A. D. Ball, A new method of accurate broken rotor bar diagnosis based on modulation signal bispectrum analysis of motor current signals, Mechanical Systems and Signal Processing. 50 (2015) 400-413.

[31]. Powrie, H. E. G., Fisher, C. E., Tasbaz, O. D., & Wood, R. J. K., Performance of an electrostatic oil monitoring system during an FZG gear scuffing test, International Conference on Condition Monitoring, University of Wales, Swansea, UK, (1999) 145-155.

[32]. Proctor, Margaret P., Fred B. Oswald, and Timothy L. Krants. Shuttle rudder/speed brake power drive unit (pdu) gear scuffing tests with flight gears. Glenn Research Center, Cleveland,OH, United States, Tech. Rep. NASA/TM—2005-214092, 2005.

[33]. Castro, J., and J. Seabra, Global and local analysis of gear scuffing tests using a mixed film lubrication model, Tribology International. 41 (4) (2008): 244-255.

[34]. Klein, Mark Andrew, An experimental investigation of materials and surface treatments on gear contact fatigue life, The Ohio State University, Columbus, 2009.

[35]. Xue, Jian-hua, Wei Li, and Caiyan Qin, The scuffing load capacity of involute spur gear systems based on dynamic loads and transient thermal elastohydrodynamic lubrication, Tribology International. 79 (2014) 74-83.

[36]. Ganti, Venu, Yogesh Dewangan, Saurabh Arvariya, and Shyamsananth Madhavan, Influence of Micro-Geometry on Gear Scuffing, SAE Technical Paper. 2015-26-0187, 2015.

[37]. Zhang, Jiwang, Wei Li, Huaqiang Wang, Qingpeng Song, Liantao Lu, Wenjian Wang, and Zhongwei Liu, A comparison of the effects of traditional shot peening and micro-shot peening on the scuffing resistance of carburized and quenched gear steel, Wear. 368-369 (2016) 253-257.

[38]. Alwodai, Ahmed, Fengshou Gu, and A. D. Ball, A Comparison of Different Techniques for Induction Motor Rotor Fault Diagnosis, Journal of Physics: Conference Series. 364 (1) (2012) 1-11.